



# Detector efficiency calibration using $^{88}\text{Rb}$ point source

C. Coşar<sup>1</sup> · A. Luca<sup>2</sup>

Received: 29 September 2023 / Accepted: 26 March 2024 / Published online: 26 April 2024  
© Akadémiai Kiadó, Budapest, Hungary 2024

## Abstract

A coaxial type HPGe detector, and two lanthanide scintillation type detectors have been modeled and characterized by means of Monte Carlo method implemented using the MCNP code. The isotope of interest is  $^{88}\text{Rb}$  which decays with energies up to 5 MeV, and can in theory aid in extending the efficiency calibration of the installations of interest in higher gamma rays energies. An  $^{152}\text{Eu}$  point source was used for the experimental validation of the MCNP models and excellent agreement was observed between the experimental data and the simulated data of both  $^{152}\text{Eu}$  and  $^{88}\text{Rb}$  point sources. After the experimental validation of the model, the efficiency calibration was extended for three different source-to-detector distances and the results are presented in this work.

**Keywords** MCNP · Gamma-ray spectrometry · Radiation detectors efficiency

## Introduction

With any new nuclear installation, it is important for the installation commission to have tools ready to perform the calibrations and also to improve upon old techniques by complementing with the new ones to offer enhanced capability of the facility and its instrumentations in order to perform at the highest level of quality. In this paper we propose a novel technique of extending the calibration in efficiency of three detector type (HPGe,  $\text{LaBr}_3(\text{Ce})$ , and  $\text{LaCl}_3(\text{Ce})$ ) by the use of MCNP simulations combined with Fitpeaks Gamma Analysis Software and EFFTRAN coincidence corrections. The detectors used can be found in any metrological gamma-ray spectrometry system and will be employed to standardize radionuclides at new nuclear installations alongside various radioactive sources. The first step was to employ the use of a well known radioisotope used in metrology, Europium ( $^{152}\text{Eu}$ ), measured at a known distance from the detector in an experimental setup which is described in Materials and Methods. To complement the experimental technique we

performed MCNP simulations of the three detectors experimental setup, and we employed point sources for simplicity and to further reduce possible interferences. In both the experimental and simulations. The experimental technique is complemented by the simulations aiming to extend the efficiency calibration curves. For this purpose, a Rubidium isotope was used, namely  $^{88}\text{Rb}$ , which emits gamma-rays up to 5 MeV.

Table 1 shows the decay lines that were recorded following simulations in MCNP, also these peaks have been reported in previous works which dates back 1974 and have been tabulated in ENSDF [1, 2]. Not all the lines have been used, in the Supporting information file are given the exact lines employed in this exercise.

This instrumental technique aims to enhance the existing measurement capability of the gamma-ray system in terms of efficiency calibration of various detection techniques employed in nuclear physics, nuclear engineering, medical devices and nuclear astrophysics studies[3–7].

The development of efficiency calibration techniques in gamma-ray spectrometry at energies higher than 2 or 3 MeV is not straight forward and requires taking into consideration the increase in probability of pair production effect which is affecting the measurements of radioisotopes employed for calibration of the detection setup.

The coincidence-summing effects can alter the integral of the full energy peak (FEP), impacting the efficiency value and the derived activity is being corrected and compensated.

✉ C. Coşar  
ciprian.cosar@gmail.com

<sup>1</sup> Faculty of Physics, University of Bucharest, Nr. 405 Str. Atomiştilor, Măgurele, Romania

<sup>2</sup> National Institute of R&D for Physics and Nuclear Engineering-Horia Hulubei (IFIN-HH), P.O.Box MG-6, 077125 Bucharest-Magurele, Romania

**Table 1** Decay lines of  $^{88}\text{Rb}$ 

Nr. Crt	Energy (keV)	Intensity (per 100 gamma-rays)	Half-life (seconds)	Activity (Bq)
1	898	14.0400	1066.8	10,000
2	1836	21.4000		10,000
3	2118	0.4220		10,000
4	2577	0.1800		10,000
5	2677	1.9580		10,000
6	3009	0.2440		10,000
7	3218	0.2100		10,000
8	3486	0.1310		10,000
9	4742	0.1430		10,000

Coincidence-summing arises when two or more  $\gamma$ -rays are emitted from a single decay and are detected at the same time. Moreover, other radiation such as  $\beta^-$  particles and their bremsstrahlung, X-rays (from electron capture or internal conversion), and annihilation radiation from  $\beta^+$  decay also can be in coincidence with the  $\gamma$ -rays. It is evident that the coincidence-summing is a phenomenon that should be considered when gamma radiation analysis is performed. It has been demonstrated in the works [7–12]. In this work coincidence summing is treated with the EFFTRAN code [13–17]. However, the code has not been developed for energies higher than 3 MeV.

For further enhancing of our results we employed software for quantitative and qualitative analysis in gamma-ray spectrometry analysis of spectra such as Fitzpeaks to provide the FEP activity. Fitzpeaks is an automated software which deals with finding peaks in gamma-ray spectra, this removes a great deal of work and provides a faster way to obtain the activity per photopeak, given that most radionuclides emit multiple peaks such in the case of  $^{88}\text{Rb}$  dealing with numerous peaks Fitzpeaks removes the possible human error. The software itself is capable of automatically provide efficiency calculation and calibrate the detector data based on the correction factors, all is required by the user is to supply high quality data for coincidence correction and activity of the radionuclides in the sample [18–22].

There are some limitations to the capabilities of today software employed in qualitative analysis of gamma-rays experiments, namely the coincidence summing corrections effects which is treated with EFFTRAN code in present work. The code has not been developed for energies higher than 3 MeV, this requires future work in this area, and possibly for outstanding discoveries in the field of metrological science. The codes in general have been developed for day to day operations in the nuclear field (nuclear power stations, nuclear forensics, environmental protection, medical establishments, etc.) than for some exotic experiments, the nature of day to day operations do not exceed the capabilities of softwares currently available, while going upwards

in energy like present work proposes means that the softwares requires updates and improvements in some places to address new scientific discoveries sometimes is possible for free and open source codes while other don't present useful information on the availability of user to customize the software [3–12].

## Materials and methods

### Experimental point source of Europium

A point source with  $^{152}\text{Eu}$  isotope has been experimentally measured and simulated. In the previous measurement the  $^{152}\text{Eu}$  activity was  $12,992 \pm 3\%$  Bq measured on the 10/03/2021, a new measurement for this paper was performed on the very same setup as previously employed with the same prepared source of  $^{152}\text{Eu}$  but taking into account the decay correction and the new activity for the radionuclide of  $^{152}\text{Eu}$  is  $11,719.15 \pm 3\%$  on the date of measurement 15/03/2023 [7, 32].

### Simulated rubidium point source

Rubidium source is difficult to obtain and measure so we refrain to only simulate the data for Rubidium using the MCNP code.

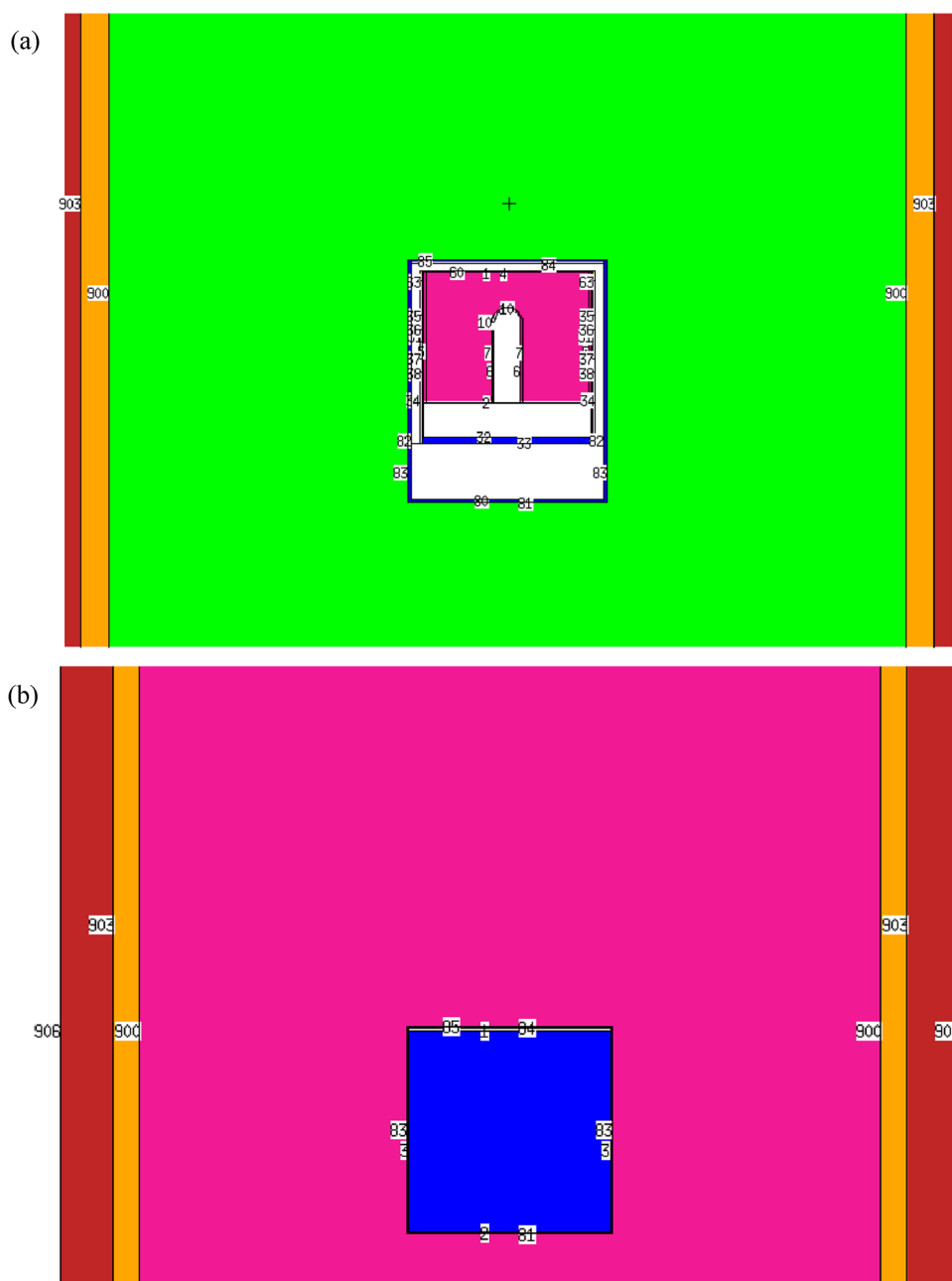
Figure 1a and b shows side view of HPGe and Scintillation detectors type  $\text{LaBr}_3(\text{Ce})$  and  $\text{LaCl}_3(\text{Ce})$  using MCNP plotter window [32].

Used in generating our data was MCNP 6.2, with both Doppler Broadening and Gaussian Energy Broadening active [1, 2, 23–25].

SUPERSynth is an easy-to-use interface to build up the MCNP input card [26].

We started by experimentally measuring an  $^{152}\text{Eu}$  source at 5 cm from a P-type coaxial HPGe detector by ORTEC—AMETEK. The source was employed experimentally in the

**Fig. 1** HPGe P-type detector used (a) & Scintillation type detectors (LaBr<sub>3</sub>(Ce) & LaCl<sub>3</sub>(Ce)) (b)



previous work published [7], and decay corrected to the date of measurement.

The <sup>152</sup>Eu point source was then simulated in the exact geometry of the experimental set-up using the MCNP code. In order to validate the used model and verify the simulation results, efficiency data calculated experimentally and by means of Monte Carlo were compared to each other with excellent agreement.

Then we employed the Rubidium point source for validation against Europium data set. The main reasons for such comparison in the spectrum is to validate the method of obtaining efficiency calculation for higher energy points the

Europium points are being used as a validation purposes against well established metrological source.

The softwares employed: SUPERSynth interface for MCNP, Fitzpeaks for efficiency calculations and spectral analysis, and EFFTRAN coincidence correction software employed on the analyzed <sup>88</sup>Rb FEPs.

Scintillation detectors the material designed for radiation interaction is homogenous and of a single type either LaBr<sub>3</sub>(Ce) or LaCl<sub>3</sub>(Ce).

The MCNP output file was saved in the file format ORTEC (.spe) which was read with Fitzpeaks. Fitzpeaks is a gamma-ray analysis software used in both experimental

and simulated spectral data. We employed Fitzpeaks to get the FEPs areas and the efficiencies per FEPs of the spectrum [27].

For coincidence summing corrections, the EFFTRAN software was used in order to calculate the correction factors of  $^{88}\text{Rb}$  up to 3 MeV [20–22, 27–31].

For  $^{88}\text{Rb}$  data points where the correction factors have not been observed/obtained a correction factor of “1.000” was employed.

Decay lines of  $^{88}\text{Rb}$ .

The efficiency per photopeak can be calculated following this formula:

$$\varepsilon = \frac{N_{\text{meas}}}{A \cdot I_{\gamma} \cdot \text{LT}_{\text{meas}}} \quad (1)$$

$N_{\text{meas}}$  is the measured counts,  $A$  is the known activity of the source in Becquerels,  $I_{\gamma}$  is the  $\gamma$ -emission intensity

and  $\text{LT}_{\text{meas}}$  is the live-time of measurement in seconds, and finally  $\varepsilon$  is the intrinsic photopeak efficiency [8].

## Results and discussion

The present work looks at extending the efficiency calibration curves by simulating a short-lived isotope of Rubidium ( $^{88}\text{Rb}$ ) and the detectors ensemble and combine the simulation results to experimental. The data sets comprise a point source of  $^{152}\text{Eu}$  which was measured in all detectors and then simulated in the exact geometry of the experimental set-up.

The addition, the radioisotope  $^{88}\text{Rb}$  was simulated at a source-to-detector distance of 5 cm aiming to extend the efficiency data points to 5 MeV.

Tables 2, 3, 4, present the data, which are also graphically represented in Figs. 2, 3, 4, 5. Here the Rubidium data set is combined with the Europium source data set.

**Table 2** Dataset for HPGe

HPGe							
Comparison data for Rubidium and Europium @ 5 cm using HPGe							
Isotopes	Energy (keV)	Efficiency (%)	Standard Deviation	Isotopes	Energy (keV)	Efficiency (%)	Standard Deviation
$^{152}\text{Eu}^*$	121.8	2.515	0.257	$^{152}\text{Eu}^{**}$	1299.2	0.324	4.487
$^{152}\text{Eu}^{**}$	121.8	2.498	1.606	$^{88}\text{Rb}^*$	1365.7	0.324	0.257
$^{152}\text{Eu}^*$	244.7	1.776	0.257	$^{88}\text{Rb}^*$	1381.9	0.343	0.257
$^{152}\text{Eu}^{**}$	244.7	1.714	1.802	$^{152}\text{Eu}^*$	1408	0.321	0.257
$^{88}\text{Rb}^*$	338.4	1.379	0.257	$^{152}\text{Eu}^{**}$	1408	0.323	1.854
$^{152}\text{Eu}^*$	344.3	1.393	0.257	$^{152}\text{Eu}^*$	1457.6	0.285	0.257
$^{152}\text{Eu}^{**}$	344.3	1.431	1.648	$^{152}\text{Eu}^{**}$	1457.6	0.324	6.785
$^{88}\text{Rb}^*$	438.8	1.120	0.257	$^{152}\text{Eu}^*$	1528.1	0.320	0.257
$^{152}\text{Eu}^*$	444	1.234	0.257	$^{152}\text{Eu}^{**}$	1528.1	0.219	7.974
$^{152}\text{Eu}^{**}$	444	1.202	2.582	$^{88}\text{Rb}^*$	1679	0.217	0.257
$^{88}\text{Rb}^*$	484	1.099	0.257	$^{88}\text{Rb}^*$	1779.5	0.215	0.257
$^{152}\text{Eu}^*$	778.9	0.976	0.257	$^{88}\text{Rb}^*$	1797.9	0.213	0.257
$^{152}\text{Eu}^{**}$	778.9	0.876	1.918	$^{88}\text{Rb}^*$	1835.5	0.182	0.257
$^{152}\text{Eu}^*$	867.4	0.766	0.257	$^{88}\text{Rb}^*$	2118.4	0.128	0.257
$^{152}\text{Eu}^{**}$	867.4	0.765	2.859	$^{88}\text{Rb}^*$	2387.6	0.062	0.257
$^{88}\text{Rb}^*$	890.7	0.766	0.257	$^{88}\text{Rb}^*$	2577.2	0.040	0.257
$^{88}\text{Rb}^*$	897.5	0.659	0.257	$^{88}\text{Rb}^*$	2677.3	0.020	0.257
$^{152}\text{Eu}^*$	964.1	0.656	0.257	$^{88}\text{Rb}^*$	2706.9	0.088	0.257
$^{152}\text{Eu}^{**}$	964.1	0.656	1.915	$^{88}\text{Rb}^*$	2733.7	0.004	0.257
$^{88}\text{Rb}^*$	1027	0.651	0.257	$^{88}\text{Rb}^*$	3009	0.002	0.257
$^{152}\text{Eu}^*$	1085.8	0.546	0.257	$^{88}\text{Rb}^*$	3218	0.001	0.257
$^{152}\text{Eu}^{**}$	1085.8	0.548	2.150	$^{88}\text{Rb}^*$	3486	0.001	0.257
$^{152}\text{Eu}^*$	1112.1	0.545	0.257	$^{88}\text{Rb}^*$	3523.7	0.028	0.257
$^{152}\text{Eu}^{**}$	1112.1	0.546	2.034	$^{88}\text{Rb}^*$	4036	0.021	0.257
$^{88}\text{Rb}^*$	1217.5	0.545	0.257	$^{88}\text{Rb}^*$	4741.9	0.020	0.257
$^{152}\text{Eu}^*$	1299.2	0.431	0.257	$^{88}\text{Rb}^*$	4853	0.324	0.257

\*Simulated point

\*\*Experimental point

**Table 3** Dataset for LaBr<sub>3</sub>(Ce)

LaBr <sub>3</sub> Ce							
Comparison data for Rubidium and Europium @ 5 cm using LaBr <sub>3</sub> (Ce)							
Isotopes	Energy (keV)	Efficiency (%)	Standard Deviation	Isotopes	Energy (keV)	Efficiency (%)	Standard Deviation
<sup>152</sup> Eu	121.8	9.025	0.256	<sup>88</sup> Rb	1380.3	2.976	0.256
<sup>152</sup> Eu	244.7	6.983	0.256	<sup>152</sup> Eu	1408	2.864	0.256
<sup>88</sup> Rb	338.6	5.162	0.256	<sup>152</sup> Eu	1457.6	2.829	0.256
<sup>152</sup> Eu	344.3	5.617	0.256	<sup>152</sup> Eu	1528.1	2.806	0.256
<sup>88</sup> Rb	438.9	4.686	0.256	<sup>88</sup> Rb	1780.1	2.415	0.256
<sup>152</sup> Eu	444	4.563	0.256	<sup>88</sup> Rb	1835.5	2.415	0.256
<sup>88</sup> Rb	483.7	4.298	0.256	<sup>88</sup> Rb	2117	2.110	0.256
<sup>152</sup> Eu	778.9	3.941	0.256	<sup>88</sup> Rb	2578.7	1.829	0.256
<sup>152</sup> Eu	867.4	3.692	0.256	<sup>88</sup> Rb	2677.7	1.781	0.256
<sup>88</sup> Rb	897.5	3.399	0.256	<sup>88</sup> Rb	3008.8	1.269	0.256
<sup>152</sup> Eu	964.1	3.372	0.256	<sup>88</sup> Rb	3212.9	1.216	0.256
<sup>88</sup> Rb	1025	3.110	0.256	<sup>88</sup> Rb	3483.4	0.998	0.256
<sup>152</sup> Eu	1085.8	2.975	0.256	<sup>88</sup> Rb	4033.1	0.935	0.256
<sup>152</sup> Eu	1112.1	2.942	0.256	<sup>88</sup> Rb	4735.6	0.915	0.256
<sup>152</sup> Eu	1299.2	2.915	0.256				

**Table 4** Dataset for LaCl<sub>3</sub>(Ce)

LaCl <sub>3</sub> Ce							
Comparison data for Rubidium and Europium @ 5 cm using LaCl <sub>3</sub> (Ce)							
Isotopes	Energy (keV)	Efficiency (%)	Standard Deviation	Isotopes	Energy (keV)	Efficiency (%)	Standard Deviation
<sup>152</sup> Eu	121.8	9.025	0.256	<sup>152</sup> Eu	1408	2.976	0.256
<sup>152</sup> Eu	244.7	6.983	0.256	<sup>152</sup> Eu	1457.6	2.864	0.256
<sup>88</sup> Rb	338.6	5.162	0.256	<sup>152</sup> Eu	1528.1	2.829	0.256
<sup>152</sup> Eu	344.3	5.617	0.256	<sup>88</sup> Rb	1780.4	2.806	0.256
<sup>88</sup> Rb	439	4.686	0.256	<sup>88</sup> Rb	1835.4	2.415	0.256
<sup>152</sup> Eu	444	4.563	0.256	<sup>88</sup> Rb	2116.8	2.415	0.256
<sup>88</sup> Rb	483.2	4.298	0.256	<sup>88</sup> Rb	2384.2	2.110	0.256
<sup>152</sup> Eu	778.9	3.941	0.256	<sup>88</sup> Rb	2576.8	1.829	0.256
<sup>152</sup> Eu	867.4	3.692	0.256	<sup>88</sup> Rb	2677.7	1.781	0.256
<sup>88</sup> Rb	897.5	3.399	0.256	<sup>88</sup> Rb	2731.7	1.269	0.256
<sup>152</sup> Eu	964.1	3.372	0.256	<sup>88</sup> Rb	3006.1	1.216	0.256
<sup>152</sup> Eu	1085.8	3.110	0.256	<sup>88</sup> Rb	3214	0.998	0.256
<sup>152</sup> Eu	1112.1	2.975	0.256	<sup>88</sup> Rb	3484.4	0.935	0.256
<sup>152</sup> Eu	1299.2	2.942	0.256	<sup>88</sup> Rb	4028.8	0.915	0.256
<sup>88</sup> Rb	1380.3	2.915	0.256	<sup>88</sup> Rb	4729.4		

The obtained data overlaps with that of Europium source which is a clear and good indication that the whole exercise using the <sup>88</sup>Rb give credible data for efficiency curve that can be further extended and used in gamma-ray experiments at higher energies.

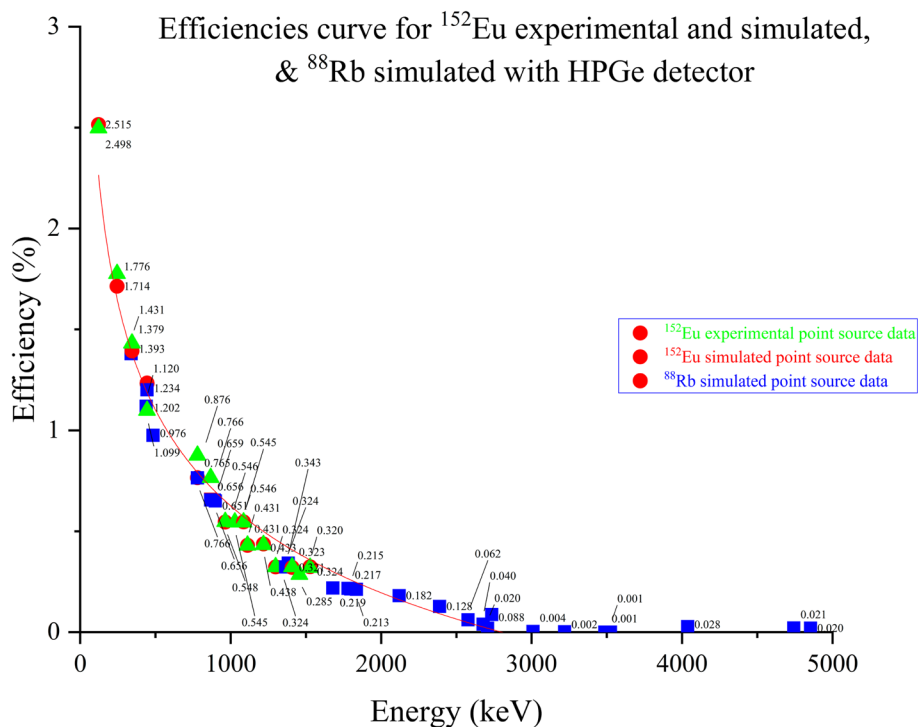
Some high energy FEPs don't have corresponding correction factor since this is not yet implemented in the software. The authors of the codes confirmed as well

that anything higher than 3 MeV is not in range of the EFFTRAN code capability [13–17]

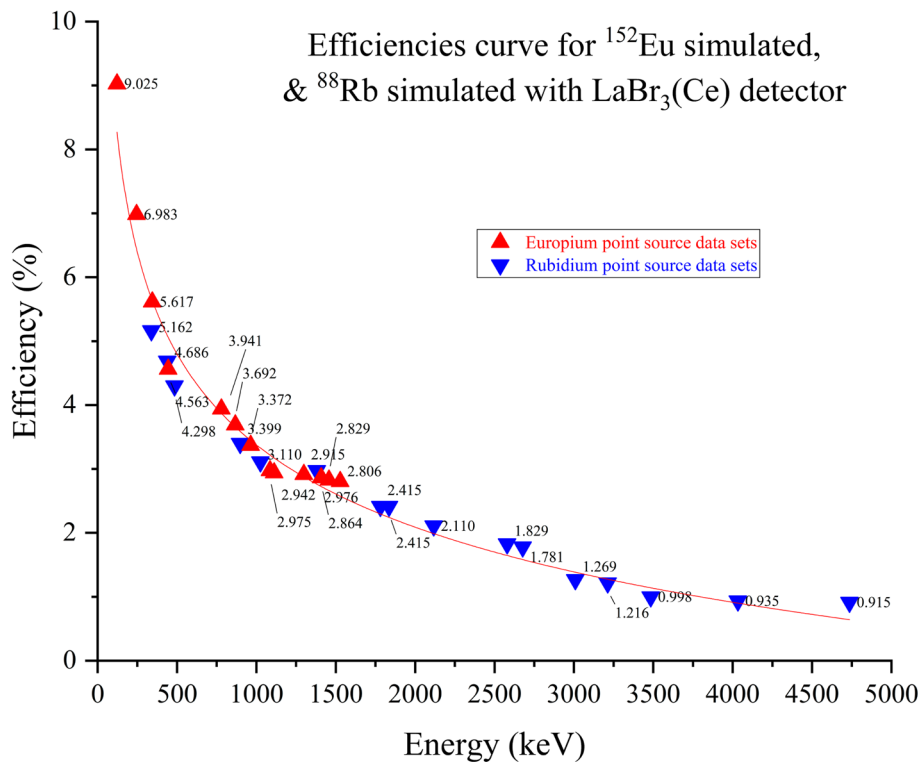
with the coincidence correction taken into account (EFFTRAN) in (%).

Figure 2 explores the combination of three different data sets, the experimental are in green for Europium source, with red the simulated data for Europium, in blue are the simulated data set for Rubidium point source.

**Fig. 2** Combined data sets for HPGe detector of the two radionuclides



**Fig. 3** Efficiencies curves from  $\text{LaBr}_3\text{Ce}$  in (%)



The efficiency curves have been fitted with a logarithmic equation of the form “ $y = a \cdot \ln(-b \cdot \ln(x))$ ” with the following coefficients  $a = 13.37723$ ,  $b = 0.11319$ . The

RMS, which in mathematics is the arithmetic mean of the squared of a data set, is calculated to 0.948.

**Fig. 4** Efficiencies curves from  $\text{LaCl}_3\text{Ce}$  in (%)

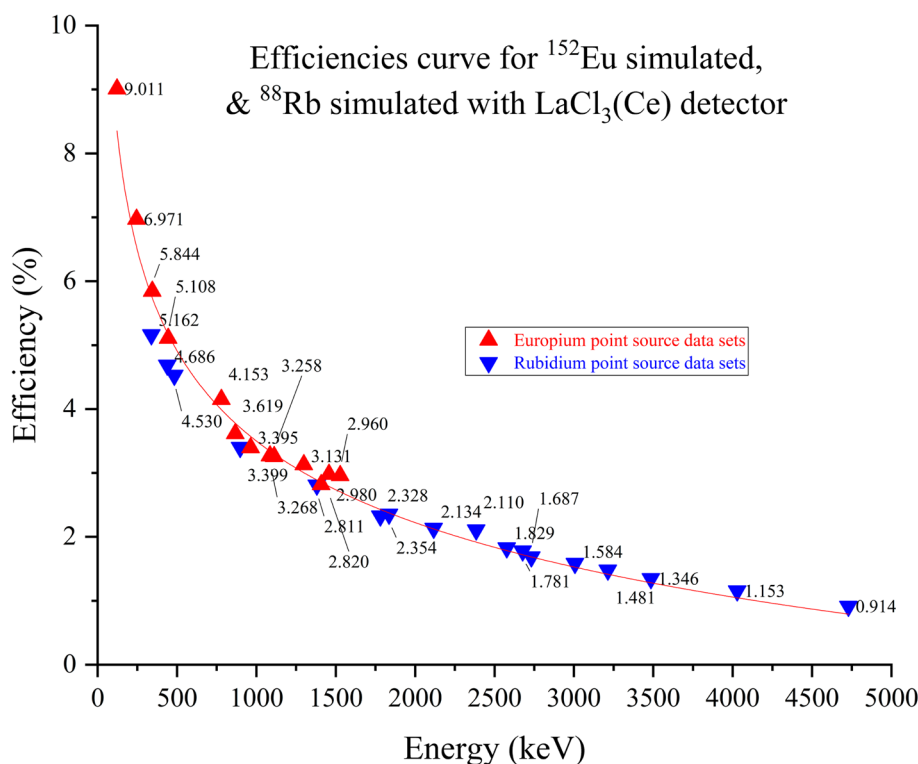


Figure 3 makes a comparison between the data obtained for  $^{152}\text{Eu}$  &  $^{88}\text{Rb}$ , for the  $\text{LaBr}_3(\text{Ce})$  detector, the data has been combined for validation and verification purpose of data points simulated. The fitted efficiency curve was of the same form as for the HPGe detector, with coefficients  $a = 13.16325$  and  $b = 0.11369$ , and the obtained RMS was 0.908.

Figure 4 makes a comparison between the data obtained for  $^{152}\text{Eu}$  &  $^{88}\text{Rb}$ , with a  $\text{LaCl}_3(\text{Ce})$  detector. The fitted efficiency curve was of the same form as for the HPGe detector, with coefficients  $a = 13.37723$  and  $b = 0.11319$ , and the obtained RMS was 0.948.

Data for Rubidium isotope and the detectors  $\text{LaBr}_3\text{Ce}$  &  $\text{LaCl}_3\text{Ce}$  have been simulated only no experimental procedure was used. The main drive behind this exercise is to develop pure computational techniques to help in with metrological measurements and validate possible other techniques implemented in the software.

In Tables 5.1, 5.2, 5.3, is the data at 10 cm, 6.1, 6.2, 6.3, is the data at 20 cm 7.1, 7.2, 7.3, is the data at 30 cm. We performed simulation at three different distances to benchmark the simulations and response of the employed softwares (FITZPEAKS, EFFTRAN and MCNP codes). Here we tracked the efficiency and the coincidence correction factors for specific distances. The data obtained coincide with the expected behaviours in term FEPs and coincidence corrections and no abnormal errors have been obtained or observed in the data.[32, 33]

In Fig. 5 we have all the lines associated with the efficiencies calibration curves for all three types of detectors. All the lines align perfectly and are being fitted with a logarithmic type equation.

## Conclusions

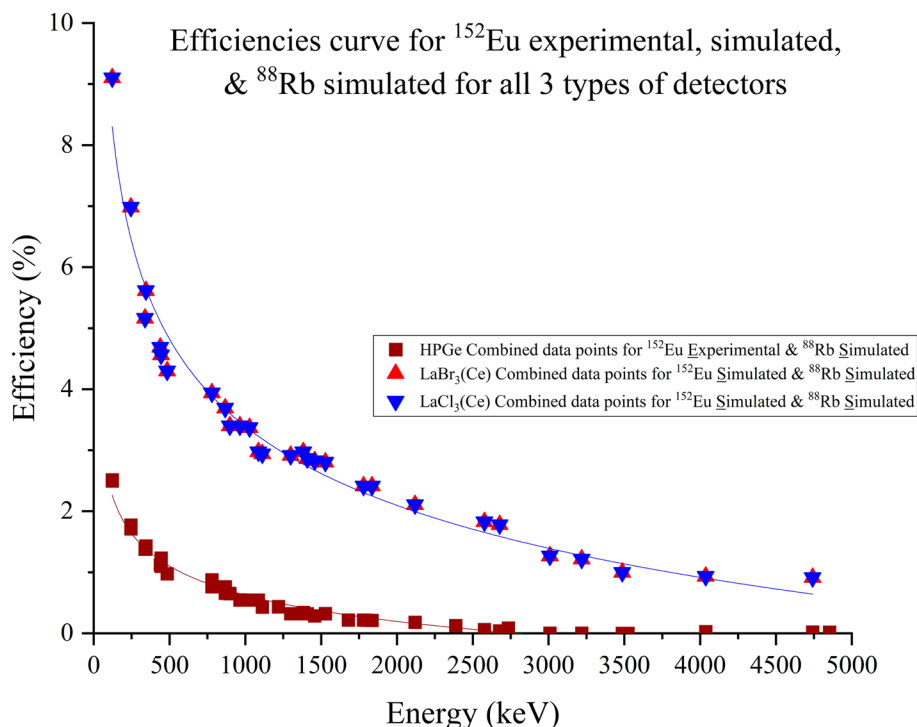
In conclusion the data obtained for  $^{88}\text{Rb}$  is in good agreement compared with experimental  $^{152}\text{Eu}$  point source data set. The efficiency curves obtained for Rubidium point source are overlapping with the efficiency data points of Europium source, some differences are being observed in the coincidence correction factors, the difference percentage is less 1%.

In all cases the fitting is being done with a logarithmic law. Logarithmic law is employed for  $^{152}\text{Eu}$  and  $^{88}\text{Rb}$  data sets and have been found in good agreement.  $^{88}\text{Rb}$  is another source much like  $^{152}\text{Eu}$  which requires taking into account the coincidence correction in the perspective of using it much like a standard source but for higher energies.

Based on the graphs data points for similar energies of both the  $^{88}\text{Rb}$  and  $^{152}\text{Eu}$  almost overlap perfectly, which gives a strong indication that the simulations results are in accordance with the obtained values of Europium.

Another remark can be concluded that we can extend from experimental values using computational techniques

**Fig. 5** Comparison of all the efficiencies curves



given the very close similarities between close values of the Europium and Rubidium, and extend the range of the efficiency calibration line to higher energies based on pure computational methods.

**Supplementary Information** The online version contains supplementary material available at <https://doi.org/10.1007/s10967-024-09478-7>.

**Data availability** All data generated or analyzed during this study are included in this published article. SI file is of xlsx type with the name SI\_Excel\_File\_Rb\_88.

## Declarations

**Conflict of interest** The authors declare that they have no known competing financial interests or personal relationships that could have appeared to influence the work reported in this paper.

## References

- Chadwick MB et al (2011) ENDF/B-VII.1 nuclear data for science and technology: cross sections, covariances, fission product yields and decay data. Nucl Data Sheets 112:2887–2996
- <https://gammaray.inl.gov/SitePages/Home.aspx>
- Erten HN, Blachot J (1974) The  $\gamma$ -ray spectrum of 17.8-min  $^{88}\text{Rb}$ . Radiochemica Acta 21:209
- Helmer & van der Lewn (2000) Nucl Inst Meth A450: 35
- Conti CC, Salinas ICP, Zylberberg H (2013) A detailed procedure to simulate an HPGe detector with MCNP5. Prog Nucl Energy 66:35–40
- Chesnevskaya S et al. (2019) Characterization of a large batch of X3 silicon detectors for the ELISSA array at ELI-NP. In: The 8th nuclear physics in astrophysics international conference
- Ntalla E, Clouvas A, Savvidou A (2018) Energy, resolution and efficiency calibration of a LaBr 3 (Ce) scintillator. HNPS Adv Nucl Phys 26:197–200
- Gilmore GR (2008) Practical gamma-ray spectrometry, 2nd edn. Wiley, London
- Ródenas J, Gallardo S, Ortiz J (2007) Comparison of a laboratory spectrum of Eu-152 with results of simulation using the MCNP code. Nucl Instrum Methods Phys Res Sect A 580:303–305
- Goodell JJ, Roberts KE (2019) Investigating the practicality of a minimally defined co-axial HPGe detector model using MCNP. J Radioanal Nucl Chem 322:1965–1973
- Debertin K, Schötzig U (1979) Coincidence summing corrections in Ge (Li)-spectrometry at low source-to-detector distances. Nucl Instrum Method 158:471–477
- Pibida L, Hsieh E, Fuentes-Figueroa A, Hammond MM, Karam L (2006) Software studies for germanium detectors data analysis. Appl Radiat Isot 64:1313–1318
- Vidmar T, Camp A, Hurtado S, Jäderström H, Kastlander J, Lépy M-C, Lutter G, Ramebäck H, Sima O, Vargas A (2016) Equivalence of computer codes for calculation of coincidence summing correction factors—part II. Appl Radiat Isot 109:482–486
- Jonsson S, Kastlander J, Vidmar T et al (2020) Experimental validation of corrections factors for  $\gamma$ - $\gamma$  and  $\gamma$ -X coincidence summing of  $^{133}\text{Ba}$ ,  $^{152}\text{Eu}$ , and  $^{125}\text{Sb}$  in volume sources. J Radioanal Nucl Chem 323:465–472
- Jonsson S, Vidmar T, Ramebäck H (2015) Implementation of calculation codes in gamma spectrometry measurements for corrections of systematic effects. J Radioanal Nucl Chem 303:1727–1736
- Vidmar T, Çelik N, Cornejo Díaz N, Dlabac A, Ewa IOB, Carrazana González JA, Hult M, Jovanović S, Lépy M-C, Mihaljević N, Sima O, Tzika F, Jurado Vargas M, Vasilopoulou T, Vidmar



- G (2010) Testing efficiency transfer codes for equivalence. *Appl Radiat Isot* 68:355–359
17. Vidmar T, Kanisch G, Vidmar G (2011) Calculation of true coincidence summing corrections for extended sources with EFFTRAN. *Appl Radiat Isot* 69:908–911
  18. Lépy MC et al (2010) Intercomparison of methods for coincidence summing corrections in gamma-ray spectrometry. *Appl Radiat Isot* 68:1407–1412
  19. Lépy MC et al (2019) A benchmark for Monte Carlo simulation in gamma-ray spectrometry. *Appl Radiat Isot* 154:108850–108850
  20. Dhibar M, Mankad D, Mazumdar I, Anil Kumar G (2016) Efficiency calibration and coincidence summing correction for a large volume (946 cm<sup>3</sup>) LaBr 3(Ce) detector: GEANT4 simulations and experimental measurements. *Appl Radiat Isot* 118:32–37
  21. Sima O, Arnold D, Dovlete C (2001) GESPECOR: a versatile tool in gamma-ray spectrometry. *J Radioanal Nucl Chem* 248:359–364
  22. Arnold D, Sima O (2000) Coincidence-summing in gamma-ray spectrometry by excitation of matrix X-rays. *Appl Radiat Isot* 52:725–732
  23. Shultis JK, Faw RE (2006) An MCNP primer. *Structure* 66506:45
  24. Werner CJ (2017) MCNP 6.2 MANUAL. Los Alamos National Laboratory, pp. 746–746
  25. Werner CJ et al. (2018) MCNP 6.2. Los Alamos National Laboratory, pp. 41–41
  26. Sima O et al (2020) Consistency test of coincidence-summing calculation methods for extended sources. *Appl Radiat Isot* 155:108921–108921
  27. Aarnio PA, Nikkinen MT, Routti JT (1992) SAMPO 90 high resolution interactive gamma-spectrum analysis including automation with macros. *J Radioanal Nucl Chem Art* 160:289–295
  28. Diago JR (2005) Simulation of detector calibration using MCNP. UpvEs. <https://www.upv.es/cherne/activities/CHERNE-sem-MC.pdf>
  29. Arnold D, Sima O (2006) Calculation of coincidence summing corrections for X-ray peaks and for sum peaks with X-ray contributions. *Appl Radiat Isot* 64:1297–1302
  30. Sima O, Arnold D (2008) A tool for processing decay scheme data that encompasses coincidence summing calculations. *Appl Radiat Isotopes* 66(6–7):705–710
  31. Sima O, Arnold D (2012) Precise measurement and calculation of coincidence summing corrections for point and linear sources. *Appl Radiat Isotopes* 70(9):2107–2111
  32. Cosar C (2023) Efficiency and coincidence benchmarking of Monte Carlo method using <sup>152</sup>Eu source. *J Radioanal Nucl Chem* 332:3009–3024. <https://doi.org/10.1007/s10967-023-08971-9>
  33. Lépy MC et al (2024) A benchmark for Monte Carlo simulations in gamma-ray spectrometry part II: true coincidence summing correction factors. *Appl Radiat Isot* 204:111109

**Publisher's Note** Springer Nature remains neutral with regard to jurisdictional claims in published maps and institutional affiliations.

Springer Nature or its licensor (e.g. a society or other partner) holds exclusive rights to this article under a publishing agreement with the author(s) or other rightsholder(s); author self-archiving of the accepted manuscript version of this article is solely governed by the terms of such publishing agreement and applicable law.